RESEARCH PAPER

CrossMark

Simulation-based investigation on the temperature influence in laser transmission welding of thermoplastics

Patrick Lakemeyer[1] · Volker Schöppner[1]

Abstract
Because of several advantages, e.g., an exact and high energy input, laser transmission welding has become more and more important in the last few years. Due to the contactless energy input, a sufficient process control is a challenge. In industrial production, the process parameters for a good weld seam are qualified by the energy input, which describes the process parameters laser power, laser velocity and irradiation time. These process parameters lead to the welding temperature, which influence the weld seam quality. The question remaining is whether the energy input describes the weld strength sufficiently or whether the welding temperature has a higher influence on the weld quality. In this study, the influence of the energy input on the weld quality is determined for an industrially relevant material combination (PBT ASA-GF20 and PC) in experimental examinations for quasi-simultaneous laser transmission welding. The welding temperature for every design point is calculated and the influence of the temperature on the weld strength is analyzed in an FEM model. In order to compare the influences of the two factors, welding temperature and energy input, a correlation analysis is performed. The correlation analysis shows a higher influence of the welding temperature on the weld strength compared to the energy input. But the energy input is also able to describe the weld strength.

Keywords Polymer joining · Thermoplastics · Thermo-mechanical FEM-model · Energy input · Laser transmission welding · Welding temperature

1 Introduction

Due to several advantages like the exact and contactless energy input, the high energy density or the high flexibility, laser transmission welding (LTW) of thermoplastics is getting more and more important [1]. Currently, the quality and control standards of the customers are increasing, which results in a high demand of an online controlling system for LTW [2]. One opportunity to control the weld quality is the measuring of the process parameters and exclusively for the quasi-simultaneous welding (QSW) the measuring of the joining displacement [3].

Currently in most applications, the weld seam quality and also the process parameters are described by the energy input and not by the welding temperature, which can be measured by recent developments [4, 5]. Especially for the machine operator it is the easiest way to describe the process parameters by one value—the energy input. Most studies about LTW deal with the energy input to describe the variation of process parameters and to analyze the results, for example the weld strength [6]. The energy input in LTW leads to a temperature profile in the weld seam. This temperature influences material properties (e.g., the degree of crystallization), thermal degradation, adhesion and diffusion between the two joining partners. So the weld seam properties result from the temperature, which depends strongly on the process parameters [7, 8]. The main question is whether the energy input describes the weld quality in a sufficient way or whether the weld quality has to be described by the resulting temperature in the weld seam. For example during QSW, the weld temperature depends on

✉ Volker Schöppner
  volker.schoeppner@ktp.upb.de

  Patrick Lakemeyer
  patrick.lakemeyer@ktp.upb.de

[1] Kunststofftechnik Paderborn, Paderborn University, Paderborn, Germany

the process parameters and the squeeze flow. So the energy input may not be sufficient to describe the weld quality.

In this study, the optimal process parameters for QSW are determined by the weld strength for an industrially used material combination. The welding temperature is calculated by a FEM model for the design points. The influence of the energy input and the welding temperature on the weld strength is analyzed and compared to each other by using a correlation analysis.

2 Quasi-simultaneous laser transmission welding

For LTW, a laser absorbing and a laser transparent part are necessary. Both parts are in contact with each other. The laser beam passes through the transparent part with a low energy loss and is absorbed in the surface layers of the absorbing part. Due to thermal conductivity, the transparent part is heated, too. The irradiation of the joining area can be conducted by several strategies: mask, simultaneous, contour, and quasi-simultaneous welding [9, 10]. QSW uses a laser spot, which is moved very fast along the weld seam (scanning speed). The fast movement of the laser beam during QSW and the relatively low thermal conductivity of plastics allow the entire weld seam to be heated at roughly the same time. The result here is a squeeze flow into the weld bead, which leads to a joining displacement. The basic process parameters for QSW are the laser power, the scanning speed and the irradiation time, which can be summarized in the energy input, and also the joining pressure [11].

3 Determination of optimal process parameters

For the experimental investigations a laser scanning system of the company ARGES GmbH (Wackersdorf, Germany) was used. The system consists of the scan head Fiber Elephant, the ASC 6 controller with an integrated 400 W fiber laser (gaussian profile) and the controlling software InScript®. The joining pressure is applied by a pneumatic cylinder. Figure 1 illustrates the American Welding Society (AWS) specimens used and the laser path. The absorbing joining partner is made of Ultradur S 4090 (PBT ASA GF20) and the transparent part is made of Makrolon AL 2447 (PC). The focus position is 320 mm behind the joining plane. The spot diameter increases with the laser power from 7 mm (90 W) to 9 mm (225 W) and the joining pressure is constant for every design point (0.4 MPa).

In the examination, the process parameters laser power, scanning speed, and number of scans (irradiation time) were varied. The parts to be joined were irradiated quasi-
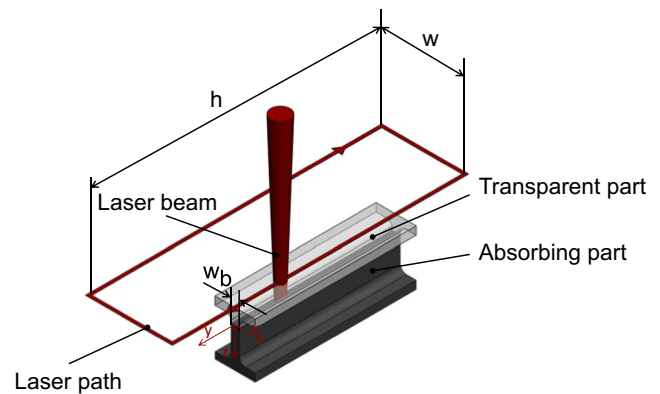

Fig. 1 AWS specimen with a rectangular laser path ($h = 110$ mm, $w = 20$ mm, $w_b = 2.6$ mm)

simultaneously with a minimum scanning speed of 3 m/s. Before measuring the tensile strength, a process window for the minimum and maximum laser power was determined. Under 90 W no sufficient handling strength could be detected. The process parameters were varied in a D-optimal design plan with the three factors laser power (4 levels), scanning speed (3 levels), and number of scans (4 levels), which can be seen in Table 1. Each design point was repeated 5 times according to DIN ISO 527.

Because of the low thermal conductivity of plastics and the high scanning speed, there was no influence of the scanning speed on the strength detected. To describe the welding conditions, the energy input was calculated for every design point by [12]:

$$E_s = N \cdot \frac{P_L}{v_s}$$

In Fig. 2, the weld strength for the four laser power levels are shown as a function of the energy input. The curve progression is the same for all laser power levels. With increasing energy input by a higher irradiation time, the strength increases too. Beyond a certain value of the energy input, the energy loss due to the squeeze flow into the weld bead is equal to the energy input. In this steady state, the welding temperature and the flow behavior are constant. As a consequence of this, the weld strength is at a constant level. This constant weld strength level is the highest for the lowest laser power (90 W). With increasing laser power, the weld strength in the steady-state phase decreases because of thermal degradation. The

Table 1 D-optimal design plan with three factors

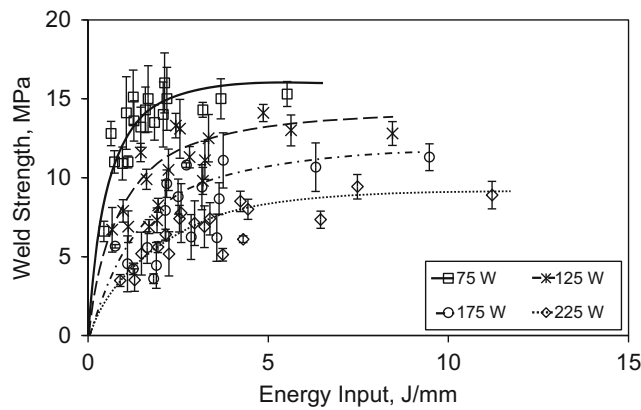| Power [W]	Scan speed [m/s]	Number of scans [−]
90	3	30
135	5	50
180	8	100
225	–	150

Fig. 2 Weld strengths for different laser powers according to DIN ISO 527 (testing speed: 5 mm/min)

same curve shape for the weld strength of QSW was determined in other studies [11, 12]. For a laser power lower than 90 W, no sufficient weld strength could be determined in the pre-screening runs. In the next paragraph, the welding temperature is calculated by a FEM simulation to show the influence of the temperature on the weld strength.

4 Simulation of the welding temperature

The simulation of the temperature profile in the weld seam was conducted with the FEM software ABAQUS. For the simulation it is necessary to specify the material properties, the laser intensity, the joining displacement, the joining pressure, the irradiation time, the laser path length, the scanning speed and the ambient temperature. The intensity distribution was measured by a charge-coupled device (CCD) camera (Ophir-Spiricon LLC: SP620U, beam splitter LBS-300) for every laser power behind the transparent AWS specimen. In QSW, the laser beam moves quickly along the weld seam. At the actual laser position, the material gets heated. All other regions cool down between scans. If the scanning speed is high enough, the cooling between scans is very small. So for the FEM model, the cooling is disregarded. The quasi-simultaneous heating is converted into a simultaneous heating with the scanning speed and the time for one scan by:

$$\overline{I}_{(x)} = \frac{1}{t_u} \cdot \int_0^{t_u} I_0 \cdot e^{-2 \cdot \frac{x^2 + v_s^2 \cdot t^2}{w^2}} dt$$

The intensity ($\overline{I}_{(x)}$) of the laser beam is assumed in the thermo-mechanical FEM model by several heat sources along the cross section. For every thermal source, the intensity distribution is averaged at the surface by:

$$\overline{I}_n = \frac{1}{\Delta x \cdot t_u} \cdot \int_{x_{n-1}}^{x t_u} \int_0^{t_u} I_0 \cdot e^{-2 \cdot \frac{x^2 + v_s^2 \cdot t^2}{w^2}} dt \, dx$$

$\overline{I}_n$ means the intensity for the heat source at the surface of the absorbing part. The intensity behavior into the absorbing part can also be characterized by the Lambert-Bourger law:

$$\overline{I}_1(z) = \overline{I}_1 \cdot e^{-K \cdot z}$$

The studied absorbing material (PBT ASA GF20) has a very low optical penetration depth of 40 μm. So the intensity curve into the absorbing material (z-direction) can be averaged over the penetration depth of 40 μm, which is applied as the several thermal sources ($\dot{\phi}_{1,1}$ to $\dot{\phi}_{13,1}$), see Fig. 3, in the model:

$$\dot{\phi}_{n,1} = \frac{1}{\Delta z} \int_0^{\Delta z} \overline{I}_n \cdot e^{-K \cdot z} dz$$

In ABAQUS, a 2D thermo-mechanical model was created to simulate the welding temperature. The model consists of three parts: the absorbing part, the transparent part, and the thermal source. The width of all parts is equal to the half width of the AWS specimen (taking advantage of symmetrical
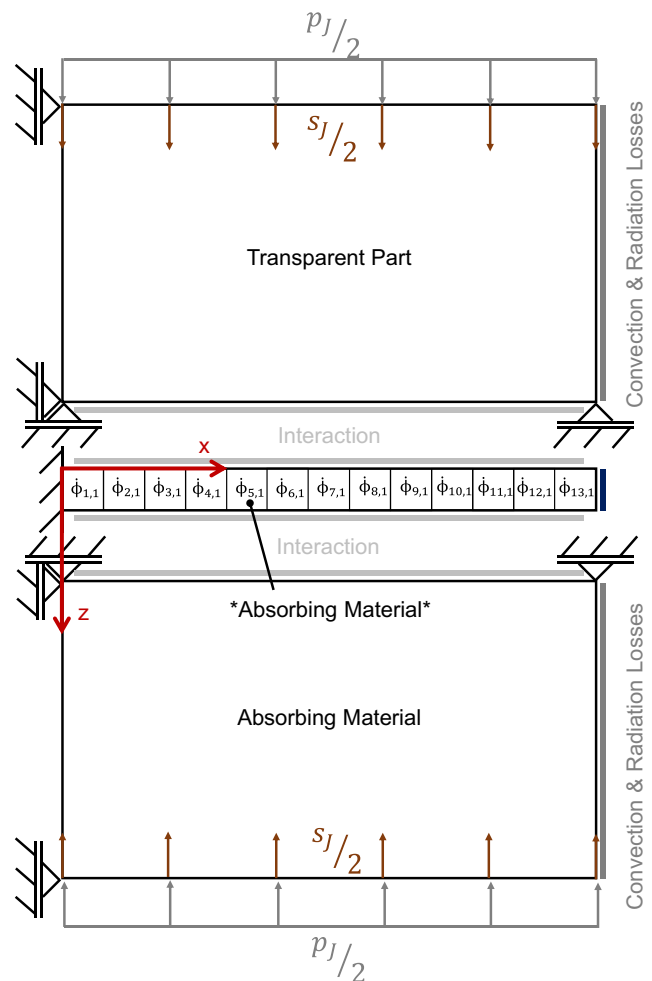

Fig. 3 2D Thermo-mechanical FEM model

conditions). To reduce the calculation time, the height of the transparent and absorbing part is 1 mm. Above 1 mm there is only low temperature during welding. The thermal source is clamped firmly by fictitious high Young's modulus (9,000,000 GPa). This high value has been chosen to avoid any displacement of the nodes. The thermal properties of the thermal source are the same as for the absorbing material. In other models [13], the mechanical properties of the thermal sources are the same as for the absorbing material. This leads to a displacement of the nodes of the thermal sources. With the displacement of the nodes, the thermal sources are changing too and the intensity distribution is not the same. For the investigated material with a very low penetration depth, the thermal source can be applied as a very small layer (40 μm) with no displacement. For the transparent and absorbing part, the mechanical properties (stress-strain characteristics for several temperature levels) of the material depend on the stress and temperature during welding. As a consequence of this, there is a displacement of the nodes, which simulates the squeeze flow in joining. This is established with the aid of the thermo-elasticity and plasticity theory. In this theory, the over-all strain ε_{all} is made up of an elastic (ε_{ij}^{el}), a plastic (ε_{ij}^{pl}), and a thermal component (ε_{ij}^{th}). When the load is removed, the plastic component remains [14]:

$$\varepsilon_{all} = \varepsilon_{ij}^{el} + \varepsilon_{ij}^{pl} + \varepsilon_{ij}^{th}$$

The transparent and absorbing parts are coupled with the thermal source by an interaction with the thermal conductance of the materials and a hard contact. The gap between the two parts and the thermal source is infinitesimally small. Besides the material properties and interactions, there are more boundary conditions applied in the model like convection or bearing, as shown in Fig. 3.

As mentioned, in QSW, there are different welding phases. In the first phase (phase I), the material is heated and starts to melt. In this phase, the material is not molten at the complete weld seam. The temperature increases, but there is only a very low settlement possible and no joining displacement. In the second phase (phase II), the complete weld seam is plasticized and due to the joining pressure a joining displacement is possible. The temperature increases, too. In the steady-state phase (phase III), the melting rate and the temperature are constant. The energy input due to the laser irradiation is equal to the energy loss of the squeeze flow. The phases in QSW are shown with the welding temperature and the joining displacement in Fig. 4 [11]. For dissimilar thermoplastic joints, the temperature in the steady state phase is above the melting temperature of the material with a higher melting point as described in Fig. 4.
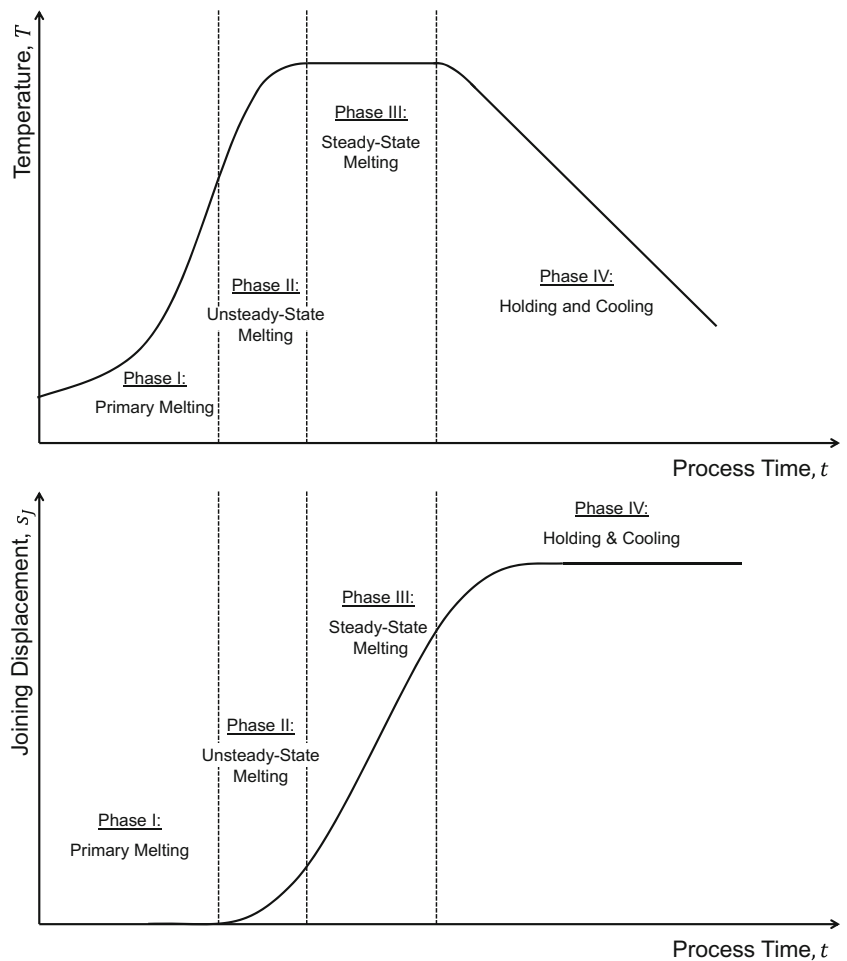
To reduce the calculation time and due to convergence problems as a consequence of the high displacement of the nodes, only the first two phases were simulated. After the second phase, the squeeze flow and also the temperature are constant. For the

design points in the steady-state phase, the temperatures at the end of phase II were used. The model is divided into three steps. The first two steps describe the phase I with a settlement of the two parts. At the end of the second step, the temperature of the node at the outside surface in the joining area ($z = 0$) has a temperature of 220 °C. This temperature is above the glass transition temperature of PC ($T_g = 165$ °C) and above the melting point of PBT ($T_m = 220$ °C). In the next step, the squeeze flow starts and at the end of this step the steady-state phase is reached. The joining displacements and the times of the several phases (step times) for the investigated laser powers were determined by measuring the joining displacement, as shown in Fig. 5. In the figure, the displacements and phase times for the phase I and II of 90 W are marked. With increasing laser power the melting rate increases, but the joining displacement at the end of the unsteady-state phase is the same for every laser power (0.4 mm). This can be explained by a more intensive squeeze flow. So the energy loss for a higher laser power is also higher. The steady-state phase is reached faster.

Due to the high joining displacement and also the high displacement of the nodes in the joining area, linear elements with reduced integration (CPE4RT) were used for meshing the part as it is proposed in [15]. To prevent problems with hourglassing, which means nonphysical modes of deformation, which occurs in underintegrated elements and produces no stress [16], a convergence test was done to specify a sufficient mesh density. In Fig. 6, the temperature profile in the contact area of the transparent and absorbing part ($z = 0$) at the end of the phase II are shown for different numbers of elements. For up to 2106 elements, the temperature profile is still the same. So a number of 2106 elements (element size: 0.05 mm) leads to sufficient simulation results. To reduce the calculation time, this mesh density was selected for the simulation.

In Fig. 7, the temperature profile for a laser power of 90 W in the steady-state phase is shown. Due to the low penetration depth of the absorbing material, the highest temperature is detected at the surface of the absorbing part in the middle of the weld seam ($x = 0$, $z = 0$). Figure 8 shows the temperature profiles for 90 W and several irradiation times. Up to 2.7 s, there is only a very small joining displacement of 0.07 mm, which means only a settlement of the two parts by the joining pressure. The squeeze flow, like it is defined in [9, 11], starts above 2.7 s irradiation time and the nodes, which are pressed into the bead, were not irradiated by the laser power. The nodes in the weld bead cool down. After 4.6 s irradiation time the steady-state phase is reached and the welding temperature is constant. Due to the very low penetration depth, the highest temperature is in the contact area of the two joining partners, which means a surface absorption. For the correlation analysis the highest temperature was selected to describe the weld quality. If the temperature exceeds the decomposition temperature the mechanical properties of the material deteriorates. So in Fig. 9, the highest welding temperature of the experimental examinations are shown depending on the

Fig. 4 Development of
temperature and joining
displacement during QSW [11]

Phase III:
Steady-State
Melting

Phase II:
Unsteady-State
Melting

Phase IV:
Holding and Cooling

Phase I:
Primary Melting

Temperature, *T*

Process Time, *t*

Phase IV:
Holding & Cooling

Phase III:
Steady-State
Melting

Phase II:
Unsteady-State
Melting

Phase I:
Primary Melting

Joining Displacement, s_J

Process Time, *t*

irradiation time and the laser power. With a higher laser power, the temperature increase is higher. Also it can be seen that a higher laser intensity leads to higher welding temperatures in the steady-state phase, which is reached faster.

To describe the thermal degradation of the material, the decomposition temperature was measured in a differential scanning calorimeter (DSC) for PBT ASA-GF20 (340 °C) and PC (400 °C). The critical temperature is 340 °C for this

material combination. Figure 10 shows the dependence of the weld strength on the calculated maximum welding temperature. The optimal welding temperature is in the range of the decomposition temperature. The high weld strength above the decomposition temperature can be explained by the determination of the temperature. The shown maximum temperature in Fig. 10 is in the middle of the weld seam. With increasing x-coordinate up to the decomposition temperature, the temperature decreases. So the main area in the welding plane is under
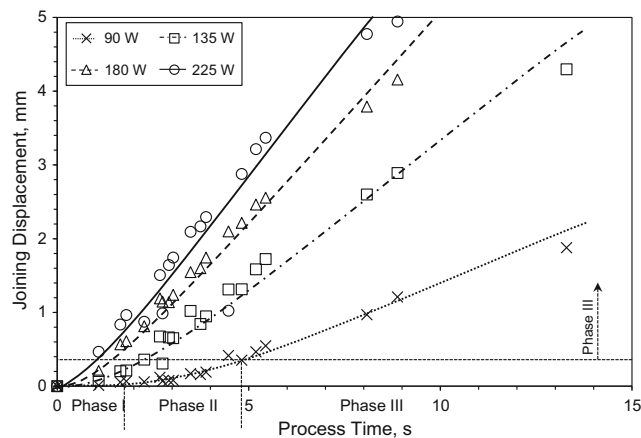

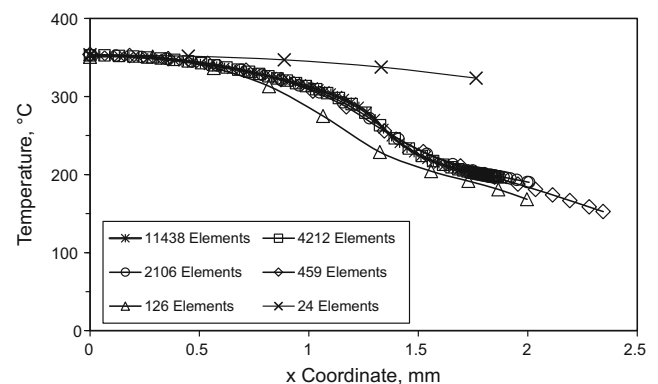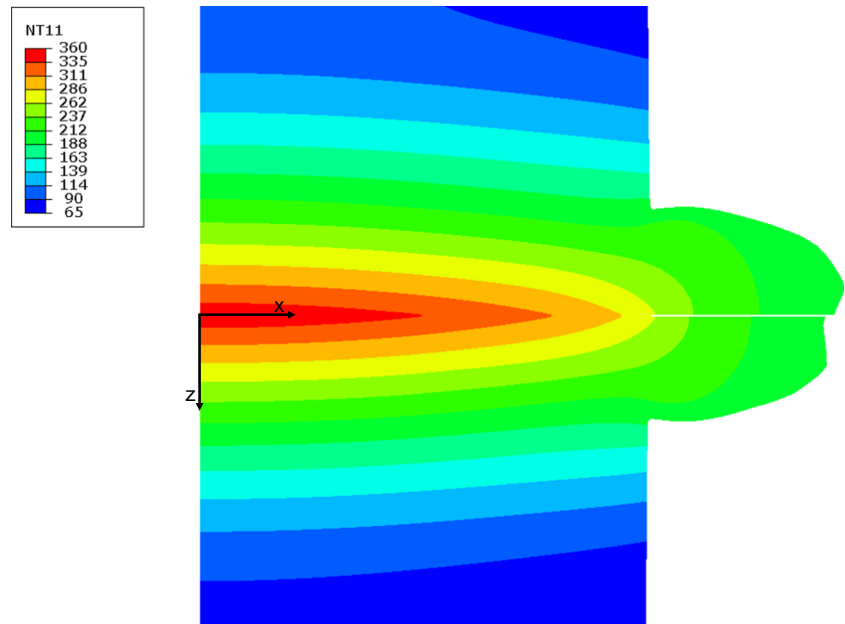**Fig. 5** Joining displacement of the experimental examinations

Fig. 6 Convergence analysis for CPE4RT elements

NT11
360
335
311
286
262
237
212
188
163
139
114
90
65

the decomposition limit. The optimal welding temperature in the range of the decomposition limit results from the agility of the polymer chains. With higher temperature, the agility of the polymer chains is higher and because of this diffusion and adhesion between the two joining parts increase, too. But temperatures appreciably above the decomposition limits lead to a thermal damage of the polymer chains. The weld strength decreases, which can be seen by the decreasing welding strength for higher temperatures.

5 Correlation analysis of the weld strength, the energy input, and the welding temperature

The main issue of this study is the question of the influence of the energy input and the welding temperature on the weld seam quality. In the preceding sections, influences of the

energy input and also the welding temperature on the weld strength were detected. To compare the influence of the energy input on the weld strength with the influence of the welding temperature on the weld strength, the Spearman correlation coefficient is calculated for the maximum welding temperature and the weld strength by [17]:

$$r_{\sigma,T} = \frac{\sum_{i=1}^{m}\left(T_{R,i}-\overline{T}_R\right)\left(\sigma_{R,i}-\overline{\sigma}_R\right)}{\sqrt{\sum_{i=1}^{m}\left(T_{R,i}-\overline{T}_R\right)2\left(\sigma_{R,i}-\overline{\sigma}_R\right)2}}$$

The Spearman correlation coefficient can be used for non-linear and/or normally distributed effects like the correlation between weld strength and energy input/welding temperature, see Figs. 2 and 10. For the calculation of the Spearman correlation coefficients, the values weld strength, welding temperature, and energy input are sorted in ascending order and assigned to ranks. For these rank values, the Spearman correlation coefficient is defined as the Pearson correlation
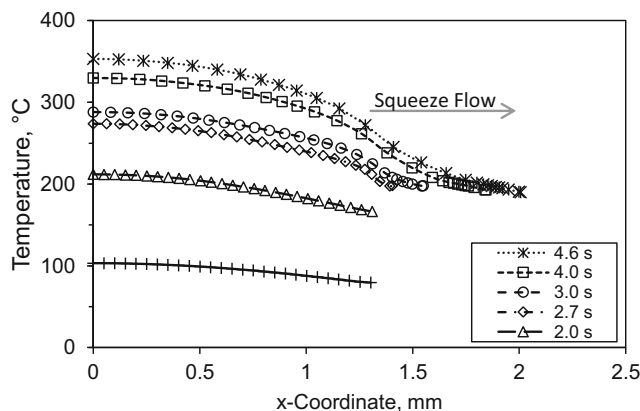

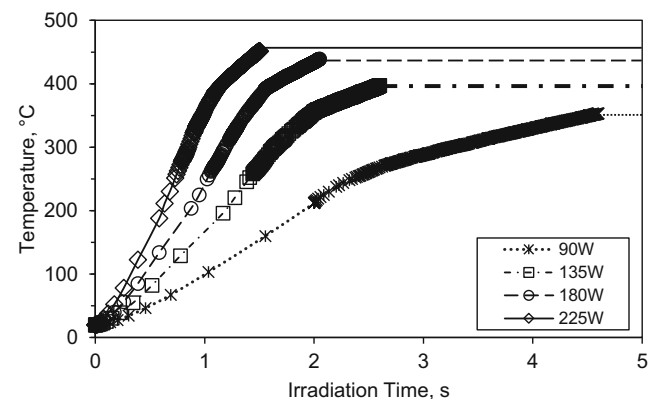Fig. 8 Temperature profile for $z = 0$ and a laser power of 90 W

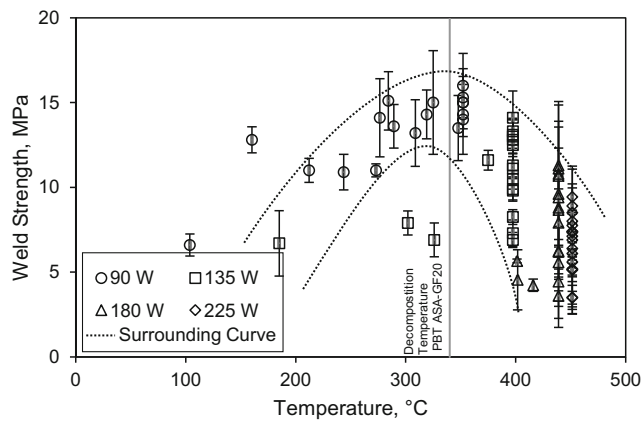Fig. 9 Maximum welding temperature in the weld seam ($x = 0$, $z = 0$)

Fig. 10 Weld strength depending on the welding temperature

Table 2 Results of the correlation analysis (influence on the weld strength)

	Temperature	Energy input
Spearman	−0.6027	−0.1129
z-value	−5.627	0.9151
Confidence interval	−5.7474	0.7947
	−5.5067	1.0355
t test ($\alpha = 0.05$)	Significant	Not significant
t test ($\alpha = 0.175$)	Significant	Significant
p value	0.0000	0.3602

coefficient for linear correlation problems [17]. The calculation of the Spearman correlation coefficient for the energy input and the weld strength is done in the same manner. To evaluate the two correlation coefficients the Fisher transformation [18]

$$F_{(r)} = 0.5*(ln(1+r) - ln(1-r))$$

and a z-transformation

$$c = \sqrt{\frac{m-3}{1.06}} * F_{(r)}$$

are conducted to calculate the confidence interval of the two correlation coefficients [18]:

$$c \pm s; s = \frac{1}{\sqrt{m-3}}$$

If the confidence intervals do not overlap each other, the correlation coefficients are independent from each other. Therefore, the energy input does not lead directly to the welding temperature. For example the joining displacement also has an influence on the welding temperature like it was determined in [12]. For proofing the significance of the correlation coefficient, the p value was determined and the t test for a confidence level of 95% and 82.5% was done with the test value of [18]:

$$t = r_{\sigma,T} * \sqrt{\frac{m-2}{1-r_{\sigma,T}^2}}$$

The correlation coefficients and results of the statistics test are shown in Table 2.

The comparison of the two correlation coefficients shows a higher influence of the welding temperature on the weld strength than the influence of the energy input on the weld strength. The correlation coefficient of the temperature is also significant for a confidence level of 95%. This can be also seen in the low p value (0.0000). The correlation coefficient

of the energy input is only significant for a confidence level of 82.5% and has a p value of 0.3602. So the correlation analysis shows also an influence between the energy input and the weld strength, but it is lower than the influence of the welding temperature. Due to other influences during welding, like the energy loss as a consequence of squeeze flow, the energy input cannot describe the weld quality exactly for the QSW. The exact weld seam properties result from the welding temperature. It must be also mentioned, that there are more factors, which influence the weld quality. For example the temperature influence time has an effect on the thermal degradation and the diffusion between the two joining partners. In this study, the temperature influence time was not analyzed because of the high melting rate of the material. So the temperature influence time is very low and also constant in the steady-state phase.

6 Conclusions

In this study, the influences of the energy input and the welding temperature on the weld quality were determined for QSW and the dissimilar thermoplastics PBT ASA and PC. In experimental examinations, it was shown that the energy input has an influence on the weld strength for these materials. For a constant laser power the weld strength increases with higher energy input. In the steady-state phase the weld strength is constant. Different laser powers lead to different weld strengths in the steady-state phase. The welding temperature was determined by a FEM model in ABAQUS. Furthermore, the maximum welding temperature for every design point was calculated. As welding temperature increases, the weld strength increases too until the decomposition temperature of the polymer is reached. Above the decomposition temperature, the thermal degradation of the polymer leads to a decreasing weld strength. To analyze the exact influence of the two factors energy input and welding temperature on the weld strength, a correlation analysis was performed. This analysis shows a higher influence of the welding temperature on the weld strength than of the energy input for a PBT-ASA and PC joint. But there is still an influence of the

energy input on the weld strength, which is able to describe the weld quality. For industrial processes the energy input can be used for the characterization of optimal process parameters, but the welding temperature is more suitable.

7 Outlook

The results of the investigations may be verified for a similar joint (e.g., PC/PC) and the contour welding. In contour welding, there is no joining displacement and as a consequence of this the energy input leads directly to the welding temperature. So energy input may have the same influence on the weld strength as the welding temperature. Also the influence of the time of temperature influence may be investigated and compared to the energy input and the welding temperature. A measurement during the welding process in industrial processes may be developed to characterize the optimal welding parameter based on the welding temperature and not only on the energy input.

List of symbols ASA, acrylonitrile-styrene-acrylonitrile; c, z-transformation; E_s, energy input; FEM, Finite element method; $F_{(r)}$, Fisher-transformation; GF, glass fiber (reinforced); I_0, maximum intensity of the Gaussian laser beam; $\overline{I}_n$, intensity of simultaneous welding at the surface for the thermal source ($\dot{\phi}_{n,1}$) in the FEM model; $\overline{I}_n(z) ::$, averaged intensity in the z-direction for the thermal source ($\dot{\phi}_{n,1}$) in the FEM model; $\overline{I}_{(x)}$, intensity of simultaneous irradiation; K, absorption coefficient; LTW, laser transmission welding; m, number of design points; N, number of scans; n, numbers of thermal sources; PBT, polybutylene terephthalate; PC, polycarbonate; P_L, laser power; p_J, joining pressure; QSW, quasi-simultaneous welding; $r_{\sigma,\ T}$, correlation coefficient of the weld strength and welding temperature; s, range of the confidence interval (z-transformation); s_J, joining displacement; t, t value; t, process time; t_u, time of one scan; $\overline{T}_R$, averaged ranked welding temperature; $T_{R,\ i}$, ranked welding temperature of the design point i; v_s, scanning speed; w, laser beam diameter; x, x-coordinate; Δx, width of the thermal source ($\dot{\phi}_{n,1}$) in the FEM model; z, z-coordinate; Δz, height of the thermal source ($\dot{\phi}_{n,1}$) in the FEM model; α, significance level; ε_{all}, all strain; ε_{ij}^{el}, elastic strain; ε_{ij}^{pl}, plastic strain; ε_{ij}^{th}, thermal strain; $\dot{\phi}_{n,1}$, thermal source in the FEM model; $\overline{\sigma}_R$, averaged ranked weld strength; $\sigma_{R,\ i}$, ranked weld strength of the design point i

References

1. Gotzmann G (2015) Aus dem Laserschwert wurde ein Universalwerkzeug; Kunststoffe 6/2015. Carl Hanser-Verlag, München

2. Horlemann S, Baudrit B, Heilig M et al (2015) Passive thermography as a non-destructive testing procedure during welding of plastics. Joining Plastics 9(2):106–113 DVS Media GmbH, Düsseldorf, (GER)

3. Laser LPKF & AG Electronics Qualitätsüberwachung und – dokumentation beim Laser-Kunststoffschweißen. Erlangen (GER)

4. Horn W (2009) A progressive laser joining method. Laser Technik Journal 1, Wiley-VCH Verlag, Weinheim

5. Schmaizl, Steger, Hierl (2015) Process-monitoring of Laser welding of thermoplastics, Laser Technik Journal 4, Wiley-VCH Verlag, Weinheim

6. Hopmann C, Poprawe R, Russek UA et al (2013) Comparison of process variants and modeling of preocesses for laser transmission welding in order to simplify the qualification and aelection of processes. Joining Plastics 3-4/2013 S:160–168, DVS Media GmbH, Düsseldorf

7. Kreimeier Sooriyapiragasam S, Hopmann C (2016) Modeling of the heating process during the laser transmission welding of thermoplastics and calculation of the resulting stress distribution. Welding in the World 60:777–791, International Institute of Welding, Berlin Heidelberg (GER)

8. Bates PJ, Okoro TB, Chen M (2014) Thermal degradation of PC and PA6 during Laser transmission welding. International Institute of Welding, 67th Annual Assembly, Seoul (KOR)

9. Potente (2004) Fügen von Kunststoffen. Carl Hanser Verlag, München

10. Ehrenstein GW (2004) Handbuch Kunststoffverbindungstechnik. Carl Hanser Verlag, München

11. Fiegler G (2007) Ein Beitrag zum Prozessverständnis des Laserdurchstrahklschweißens von Kunststoffen anhand des Quasisimultan- und Simultanschweißen. PhD Thesis, University of Paderborn, Paderborn (GER)

12. Wilke L, Schoeppner V, Potente H (2007) Weld quality in dependence of energy for the quasi-simultaneous welding process. International Institute of Welding, 60th Annual Assembly, Dubrovnik (CRO)

13. Wilke L, Potente H (2007) Comparing laser transmission principles, 65th Annual Technical Conference of the Society of Plastics Engineers (ANTEC), Cincinnati (USA)

14. ABAQUS 6.12 User's Manual: Volume 3, Dassaults Systems Simulia Corp., Providence RI (USA) (2012)

15. Wittel (2010) FEM for 4 - Eine kurze Einführung in die Finite Elemente Methode. ETH Zürich, Institut für Baustoffe, Rechnergestütze Physik der Werkstoffe, Zürich

16. Livemore Software Technology Corporation (2012) Hourglass (HG) modes, Las Positas Rd, Livermore, (CA)

17. Engelhard Spearman-Korrelation/Rangkorrelation, online-reference: http://www.crashkurs-statistik.de/spearman-korrelation-rangkorrelation/, Retrieved on 23.06.2016

18. Rasch, Friese, Hofman et al (2004) Quantitative Methoden 1. Springer Medizin Verlag, Heidelberg